Available online at www.sciencedirect.com
ScienceDirect
Trans. Nonferrous Met. Soc. China 22(2012) s181−s187
Transactions of Nonferrous Metals Society of China
www.tnmsc.cn

Development of porous medical implant scaffolds via laser additive manufacturing

SU Xu-bin[1], YANG Yong-qiang[2], YU Peng[1], SUN Jian-feng[2]

1. School of Materials Science and Engineering, South China University of Technology, Guangzhou 510640, China;
2. School of Mechanical and Automotive Engineering, South China University of Technology, Guangzhou 510640, China

Received 9 July 2012; accepted 6 August 2012

Abstract: The objective was to develop and evaluate the porous medical implant scaffolds designed via digital method and fabricated by laser additive manufacturing. A porous artificial femur model and several vessel scaffolds with customized design were created based on the widely used computed tomography (CT) technology and Pro/Engineer software, and then were obtained by selective laser melting of powdered titanium-alloy material. The fabricating results show that supports are not required with the improvement of the processability of lattice, and porous scaffolds with good interconnectivity can be fabricated. Some issues also appear, such as the low geometric accuracy of lattices. The exploited design freedom is an expected benefit in medical field due to the individual characteristic of each patient. It is expected that more scaffolds will be developed and applied in practical fields with further study on design, process and biocompatibility.
Key words: powdered materials; medical implant; porous structure; processability; rapid manufacturing

1 Introduction

For the past years, the laser additive manufacturing technologies have been applied to creating of physical prototypes from 3D digital models without the need for process planning. Recently, with the development of materials and the improvement of equipment, these technologies have been expected to directly fabricate metal components, which are used in practical fields [1]. The additive approach breaks up a complex 3D model into a series of 2D cross-sections with a nominal thickness so that it enables the direct fabrication of customized components which always have freeform surfaces and cannot be easily manufactured by conventional processes [2]. This observation promotes the expansion to the medical fields since the patients always have individual characteristics [3].

Scaffold, one type of implants in surgeries, has brought attention in recent years. One of the important reasons is that the scaffold cannot be easily obtained by using conventional processes due to the porous structure, for instance, the bone implant with pores for biocompatibility. To optimize the architecture of scaffolds for the direct fabrication, topology optimization is one of the new approaches which maximize scaffold stiffness and diffusive transport in the interconnected pores [4]. However, this optimization is only about the mechanical properties without consideration of the processability. It is reasonable that the processability should be considered when combining with materials and processes. As for materials, pure titanium or titanium alloy would be the most expected option, which has been widely used for various implants because of good biocompatibility and high mechanical strength. Many testing results show that the titanium-alloy components fabricated by laser additive manufacturing have higher tensile and compressive strengths but lower ductility in comparison with those of components manufactured by conventional processes [5,6]. Based on these progresses, the exploration of fabrication of porous scaffolds can be carried out. Among the limited reports, the biocompati-

Foundation item: Project (2012CB619100) supported by the National Basic Research Program of China; Projects (51072057, 50872035) supported by the National Natural Science Foundation of China; Project (2012M511797) supported by the China Postdoctoral Science Foundation
Corresponding author: SU Xu-bin; Tel: +86-20-87114484; E-mail: scutsxb@yahoo.com.cn

bility was preliminarily discussed, including the relationship between osteoindution and pore size, and the analogousness between porous structure and human bone, etc [7,8]. In addition, the post-processes, such as heat treatment, were investigated, mainly aiming to improve the mechanical behaviour [9]. Actually, the link of customized design with direct fabrication would be a challenging issue needed to be evaluated since the customized design should be assigned with good processability while the fabrication should be finished with customized feature. In other words, the development should be carried out in accordance with the patient's individual characteristics and the laser additive manufacturing process. This observation promotes a combination of additive manufacturing and computed tomography (CT), a widely used technology in medical, to facilitate the digital design of individual characteristics and the direct fabrication of unit cells, which will be evaluated in this work.

2 Development procedure and experimental conditions

Figure 1 shows the development procedure of customized porous implant scaffolds. It aims to obtain the customized scaffolds for surgical operation. The section information of pathological tissue is obtained by CT scan and the images are exported as Dicom file format. Then, the digital model can be restructured by processing of threshold segmentation, region growing or other operations in image processing software and is exported as STL file format. According to the digital model, doctors determine the repair solution and design the corresponding implants in CAD system since nearly every CAD system can input and output a STL file format. It is known that nearly every AM machine accepts the STL file format, which becomes a standard. Therefore, these two technologies, the CT and the additive manufacturing, are combined, and the customized implants can be directly fabricated after slicing and path manipulation. Compared with the conventional process, this digital method reduces the cycle time of design and fabrication. Furthermore, it builds the bridge for the cooperation between doctors and manufacturers.

In this work, the CT images were monitored by SOMATOM Emotion Spiral CT apparatus and imported into Mimics to restructure the original model. The design of customized porous structure was conducted in Pro/Engineer (version Wildfire 4.0) and the 3D model was imported into the additive manufacturing system. The employed system consisted of a ytterbium fiber laser with a continuous wavelength of 1090 nm, a galvanometer optical scanning system with dual axis mirror positioning scanners, and an F-theta lens with a focal distance of 163 mm. During the fabrication, a powder dispenser platform was raised up and a flexible brush spread powders to the built platform. Following the scanning paths programmed in the machine control data, the $X-Y$ scanner directed the laser beam to heat powders selectively to build a layer, and then the built platform descended a layer thickness. The machine repeated the above steps to fabricate a scaffold layer by layer.

The material used in the experiment was gas-atomized Ti6Al4V amorphous powder with granularity of 38 μm. The chemical compositions of the powdered material are listed in Table 1. During the experiment,

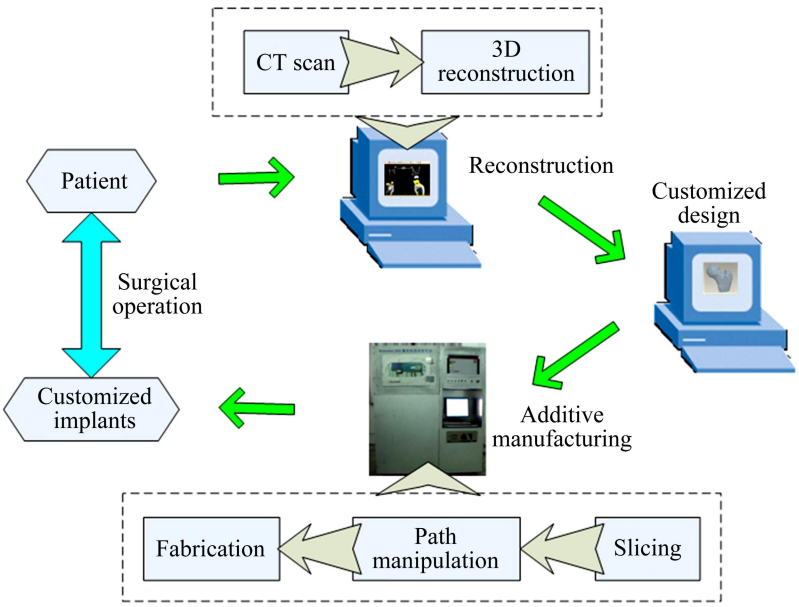

Fig. 1 Schematic of development procedure

Table 1 Chemical composition of Ti6Al4V (mass fraction, %)

Al	V	O	H	N	C	Fe	Si	Ti
5.5−6.8	3.5−4.5	0.15	0.02	0.04	0.04	0.025	0.02	Bal.

specimens were fabricated on a Ti6Al4V substrate and within an atmosphere filled up with argon as shielding gas, and the oxygen content was controlled to below 0.02%.

3 Results and discussion

3.1 Interconnectivity

Powders must not be trapped within pores, i.e., they can be removed by some methods such as high-pressure water or air when the fabrication is finished. The past research results showed that poor interconnectivity of the pores would lead to an unsuccessful reparation and pore size of about 0.5 mm suggested excellent osteoinduction [7]. Ideally, powders will not be trapped within the pores without consideration of thermal transmission since the granularity of powders is much smaller than the pore size. However, all pores must be connected to the exterior otherwise the powders cannot be removed. Therefore, the interconnectivity affects the removal of powders after fabrication as well as the tissue regeneration during reparation.

Pores are always generated by Boolean operation between the solid implant with customized surfaces and a cell cube with assigned features, which can be performed along direction *X*, *Y* or *Z*, respectively. In this way, the scaffold is endowed with 1D, 2D or 3D orthogonal pores, as shown in Fig. 2, so that the penetrability of pore facilitates the removal of powdered materials and assures good biocompatibility. Another advantage is that the elastic modulus of the artificial implant becomes smaller than the solid one. According to the simplified expression that approximately describes the relationship between elastic modulus and porosity:

$$E^* = E_0(1-\phi)^2 \quad (1)$$

where E^* is the effective elastic modulus of porous material; E_0 is the elastic modulus of full density material; and ϕ is the porosity. The scaffold will be endowed with different mechanical properties by adding of pores. This is very important in the bone repairing since the elastic modulus of most of metals is larger than that of human bone, which leads to stress shielding.

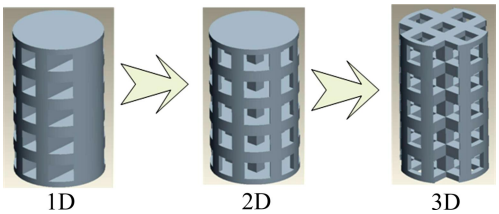

Fig. 2 Interconnectivity of porous structure

3.2 Processability

Note that even different types of pores may generate the same porosity, which implies that the structure of scaffold is diversified. This is one of the main reasons that the scaffolds can be individually designed. However, the options are good and bad when considering the processability, i.e., the fabrication quality should be considered during the design of pores. Overhang is one of the major structures affecting the fabrication quality of additive manufactured components, which always leads to some undesirable defects. When evaluating the processability, focus may be on the number of overhang structures. In particular, the control of overhangs seems more stringent when the powders are metal. The high temperature gradients between the melted material and the surroundings may lead to warpage when they are cooled. In addition, liquid-phase material droops due to gravity and capillarity, thus there will be dross formation on the overhang surface after the fabrication. Figure 3 shows a porous artificial femur model. The model is designed with orthogonal periodic pores and the pores are circular, as shown in Fig. 3(a). The pictures of the fabricated model after post-process of high-pressure air show that the powders on the upper pores are totally cleaned off, yet the powders on the lateral pores are not removed. It can be seen that the laser deep penetration almost fully melt the powders under the struts, leading to serious adhering slag.

To avoid the defects due to overhang, support structures are always added. Even though powders can offer self-support in many powder-based systems since the powder bed may be a sufficient support material for the polymer process, support structures are always needed to support overhangs during the metal fabrication and provide a starting point for the overhangs. There are also some approaches to improve the processability, such as decreasing the critical fabrication angle by adjusting the laser energy input, but adding supports is one of the major approaches since it can avoid the fluctuation of fabrication quality due to the adjustment of process parameters [10]. The supports are removed when the fabrication process is finished. The removal of too many supports may destroy the surface. The problem is that the removal of supports is not available since the pore size is

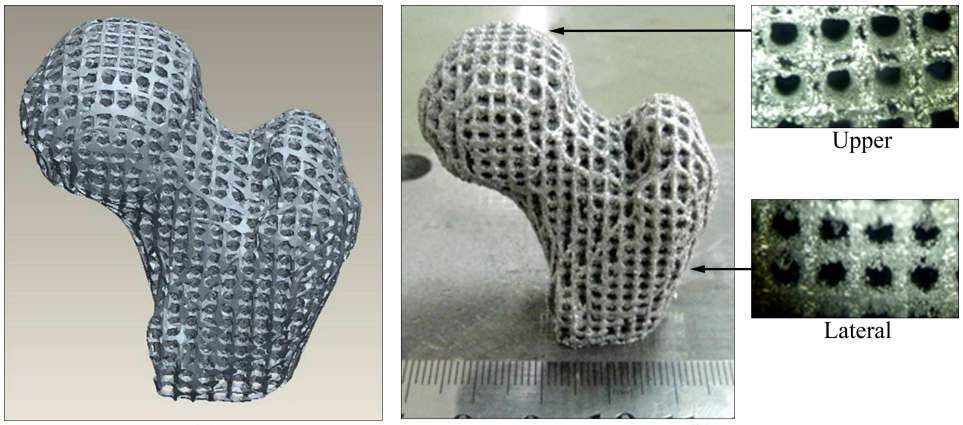

Fig. 3 Porous artificial femur model: (a) Digital model; (b) Fabricated model

small and there is not enough space within the scaffold for the tooling operation. Therefore, support structures cannot be added within the interior structures otherwise the remnant supports and the materials trapped by the supports may lead to failure fabrication.

The above discussion implies that the processability of lateral pore should be evaluated when preparing for the fabrication. As for a circular pore shown in Fig. 4(a),

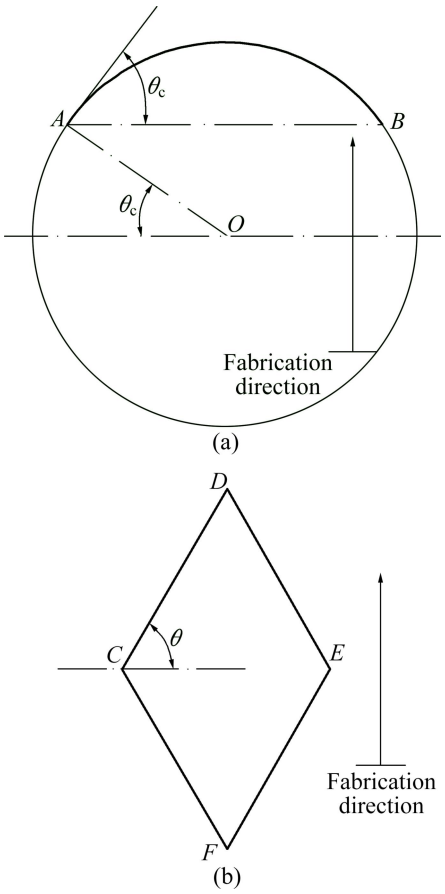

Fig. 4 Processability of lateral pore: (a) Circular pore; (b) Improved pore

suppose the critical fabrication angle is θ_c under the according process condition, arc $\overset{\frown}{AB}$ can be regarded as an overhang structure along the marked fabrication direction and supports are needed, which cannot be easily removed and eventually leads to failure fabrication, as discussed above. Making an improvement of the pore, octahedral lattice is proposed and the lateral schematic is shown in Fig. 4(b). When the fabrication angle θ of the down-facing surface "*CD*" is larger than the critical fabrication angle θ_c, the supports are not needed. The fabrication order of the lattice is as: firstly strut "*CF*" and strut "*EF*", then strut "*CD*" and strut "*DE*". The lower half of the lattice is fabricated upon point *F* and then provides starting points for the upper half.

3.3 Fabricating process

During the fabrication, a component is added layer by layer and a layer is built by track overlapping. Actually, a fabricated track is performed by the movement of focused laser spot along the scanning direction. The fusion zone within the spot, in a term of molten pool, solidifies as soon as the spot leaves. The bottom line of the molten pool is similar to a parabola because of the Gaussian distribution of laser energy of the laser beam, as shown in Fig. 5. To produce continuous solidity, the molten pool always consists of two portions: the upper portion I from powder layer and the lower portion II from the previous solidification (or substrate for the first layer). During the solidification, the heat conduction is the main transmission since the convection and the radiation can be ignored due to the laser rapid solidification. The shape of the molten pool is mainly dependent on the interfacial tension. According to elastic equation, for the equilibrium state, the interfacial tension of liquid-solid interface should be as

$$\cos\theta^* = \frac{\gamma_{sg} - \gamma_{sl}}{\gamma_{lg}} \tag{2}$$

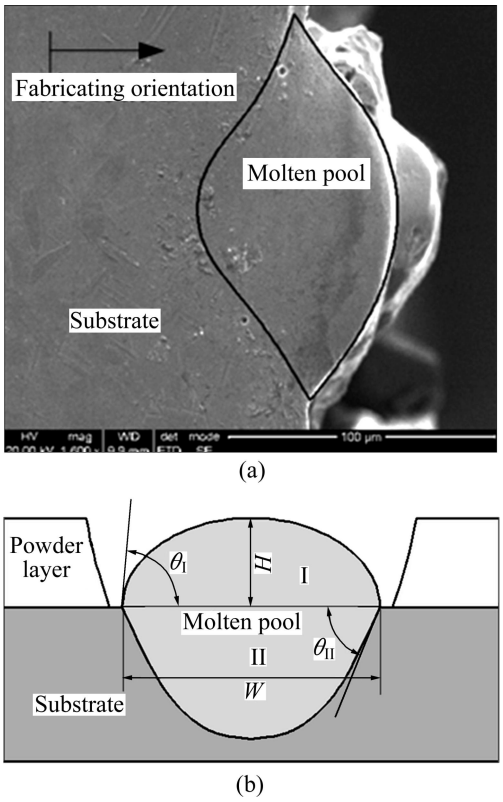

Fig. 5 Cross section of single track fabricated by SLM: (a) Micro morphology; (b) Schematic

where θ^* is the contact angle and γ_{sg}, γ_{sl} and γ_{lg} are the interfacial tensions of solid−gas interface, solid−liquid interface and liquid−gas interface, respectively. Actually, the elastic equation can only describe the shape of the molten pool in the equilibrium state, but the solidification is dynamic and the formation of the molten pool is dependent on the adhesion work from the interface. The two contact angles, θ_I of liquid−gas interface of portion I and θ_{II} of solid−liquid interface of portion II produce a bowl-shaped cross section of single track eventually.

According to the fabricating pattern of laser additive manufacturing, molten pool is the primitive element and the shape will be an important factor affecting the ongoing fabrication. Geometrically, both the contact angle and the dimensions (width and height or depth) of the molten pool can characterize the shape of cross section of fabricated track, yet the former is always difficultly measured. In addition, the width and the height, presented by W and H respectively, imply some possible fabrication defects, such as balling effect [11]. To take an insight into the dimensions of the fabricated track, the absorbed energy should be considered, which is affected by many factors. Besides the physicochemical properties of the powdered materials, the process parameters are the foremost factors needed to be considered, mainly characterized by laser power, scanning speed, track space, and layer thickness. Suppose the energy input per volume is represented by ψ, then [12]:

$$\psi=P/(vSh) \tag{3}$$

where P is the laser power; v is the scanning speed; S is the track space; and h is the layer thickness. Thus, the energy input can be characterized by P/v (unit: J/mm) when other parameters are constant. This classification is challenging since the track space and the layer thickness as well as the width and the height mentioned above can be regarded as elements characterizing the geometry of the fabricated result. When the track space and layer thickness are assigned before the fabrication, adjusting the laser power or the scanning speed brings about the fluctuation of the width and the height, leading to different surface morphologies due to the fluctuation of track overlapping.

As for the selection of process parameters, orthogonal experiment is always employed. The previous experiments show that the components fabricated from 316L stainless steel powders have a steady quality with high relative density under a group of parameters as follows: laser power of 150 W, scanning speed of 600 mm/s, track space of 0.12 mm, layer thickness of 0.035 mm, and scanning strategy of inter-layer stagger scanning [13]. In this experiment, a specimen was fabricated from Ti6Al4V powders by using the same process strategy. Figure 6 shows surface morphologies of the specimens of 316L stainless steel and Ti6Al4V. The continuity of fabricated tracks of 316L stainless steel specimen is obviously more stabilized. Whereas the surface morphology of Ti6Al4V specimen is irregular, even without any fabricated track that can be seen. Seemingly, this contrast verifies that the similar process strategy leads to a slight over-fusion. However, the interesting thing is that the fusion point of Ti6Al4V is higher than that of 316L stainless steel, thus, the needed energy input should be larger under the given condition. This phenomenon can be explained by the poor thermal conduction of Ti6Al4V. The accumulated energy makes the fabricated tracks variegate and eventually generate a worsened final surface. To avoid the accumulation of energy, increasing the scanning speed is one of the solutions [14]. Another benefit is that the fabricating efficiency is improved, i.e., the fabricating speed is increased, so that the temperature difference between the previous solidification and the current layer is decreased. The low temperature gradient between melted material and the surrounding is conducive to avoiding of warpage as it is cooled.

According to the above discussion, several vessel scaffold models were developed, as shown in Fig. 7. The

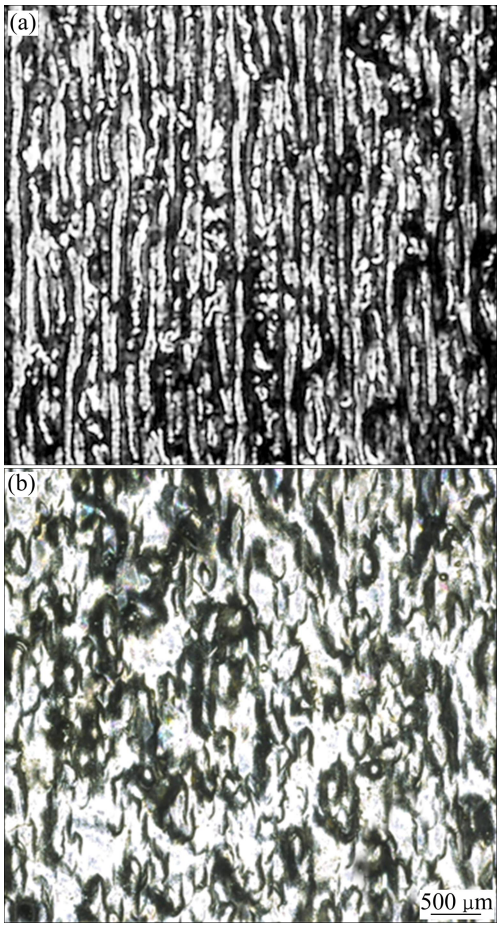

Fig. 6 Surface morphologies of fabricated specimens: (a) 316L stainless steel; (b) Ti6Al4V

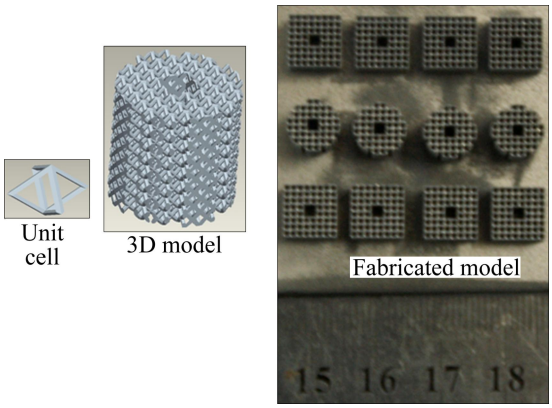

Fig. 7 Developed vessel scaffold models

unit cell was regular octahedral lattice, and two types of scaffold, cylinder and cuboid respectively, were created by Boolean operation. The process strategy mentioned above was used except for a scanning speed of 800 mm/s. The models were fabricated without addition of any support structure and each lattice was built upon the peak of the previous lattice (the bottom lattices were upon the substrate). After cutting off from the substrate by wire cutting, the models were put into a glass cup with alcohol and they were cleaned by using ultrasonic cleaning for 5 min.

SEM image in Fig. 8 shows that the residual powders within the pores are removed. However, some powders still stick on the struts. These powders are partly or even fully melted. Note that the strut size is always small, the focused laser spot may affect the geometric accuracy. According to the following expression:

$$D_{min}=(4\lambda M^2 f)/(\pi n D_0) \quad (4)$$

where D_{min} is the theoretical minimal focused laser spot size, λ is the optical wavelength, M is the beam quality, f is the focal distance, n is the expanding factor, and D_0 is the waist diameter before expanding, the focused laser spot size can be figured out. However, this calculation is carried out without consideration of the influence of the optical system and the transferred heat. The actual laser spot size used in this experiment is about 70 μm, which is obtained by measurement of the width of a scanned track on a substrate without powders. This value is much smaller than the strut size, yet the really existing powders show that the geometric accuracy becomes deteriorated. It is known that the dimensional accuracy can be improved by suitable spot compensation but the transferred heat still leads to sticking of powders on the struts, affecting the accuracy. Actually, if the powders nearby the struts are fully or partly melted, even a random powder sticking on the struts may lead to an absolute error larger than the average particle size. The profile of the pores will become smooth by adding a scanning line along the contour during the path manipulation. An additive scanning can re-melt the rough layer of the surface and create condition for the re-distribution of melted materials [15,16]. However, as for the implant scaffolds, the pores and the struts are small and there is a requirement of biocompatibility, thus the re-melting process needs to be optimized in the further experiments.

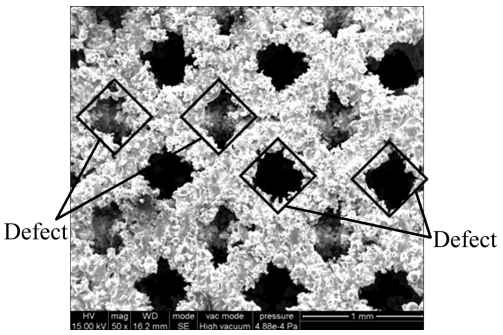

Fig. 8 Defects of fabricated scaffold

4 Conclusions and ongoing study

1) Implant scaffold can be designed with customized pores and good interconnectivity according

to the individual characteristic of patient. During the design stage, the processability of lattice needs to be evaluated. Octahedral lattice has better processability compared with the circular one.

2) Porous implant scaffold with good processability can be directly fabricated by laser additive manufacturing process without any addition of support structures. During the fabrication, the transferred heat causes sticking of powders on the struts and these powders are not easily removed by high-pressure air or ultrasonic cleaning. The profile of pores should be further improved.

3) The current research has only explored some issues during the development of implant scaffold. In the further research progress, more types of scaffold with more design freedoms will be developed, but before the scaffolds are used in the clinical practice, the improvement of process parameters and the test on biocompatibility need to be further carried out.

Acknowledgment

The contribution of Dr. WANG Di in this work is appreciated.

References

[1] GIBSON I, ROSEN W, STUCKER B. Additive manufacturing technologies [M]. New York: Springer Science and Business Media, 2010: 120−133.

[2] SCHLEIFENBAUM H, MEINERS W, WISSENBACH K, HINKE C. Individualized production by high power selective laser melting [J]. CIRP Journal of Manufacturing Science and Technology, 2010, 2: 161−169.

[3] GIANNATSIS J, DEDOUSSIS V. Additive fabrication technologies applied to medicine and health care: A review [J]. International Journal of Advanced Manufacturing Technology, 2009, 40: 116−127.

[4] CHALLIS J, ROBERTS P, GROTOWSKI F, ZHANG L, SERCOMBE B. Prototypes for bone implant scaffolds designed via topology optimization and manufactured by solid freeform fabrication [J]. Advanced Engineering Materials, 2010, 12(11): 1106−1110.

[5] CHLEBUS E, KUZNICKA B, KURZYNOWSKI T. Microstructure and mechanical behaviour of Ti−6Al−7Nb alloy produced by selective laser melting [J]. Materials Characterization, 2011, 62: 488−495.

[6] FACCHINI L, MOLINARI A, HOGES S, WISSENBACH K. Ductility of a Ti−6Al−4V alloy produced by selective laser melting of prealloyed powders [J]. Rapid Prototyping Journal, 2010, 16(6): 450−459.

[7] FUKUDA A, TAKEMOTO M, SAITO T. Osteoinduction of porous Ti implants with a channel structure fabricated by selective laser melting [J]. Acta Biomaterialia, 2011, 7: 2327−2336.

[8] PATTANAYAK K, FUKUDA A, MATSUSHITA T. Bioactive Ti metal analogous to human cancellous bone: Fabrication by selective laser melting and chemical treatments [J]. Acta Biomaterialia, 2011, 7: 1398−1406.

[9] HASAN R, MINES R, FOX P. Characterization of selectively laser melted Ti−6Al−4V micro-lattices struts [J]. Procedia Engineering, 2011, 10: 536−541.

[10] SHANG Xiao-feng, LIU Wei-jun, WANG Wei, WANG Zhi-jian. Slope limit of part made in metal powder laser shaping [J]. Chinese Journal of Mechanical Engineering, 2007, 43(8): 97−100. (in Chinese)

[11] GUSAROV V, YADROITSEV I, BERTRAND P, SMUROV I. Heat transfer modeling and stability analysis of selective laser melting [J]. Applied Surface Science, 2007, 254(4): 975−979.

[12] SIMCHI A. Direct sintering of metal powders: Mechanism, kinetics and microstructural features [J]. Materials Science and Engineering A, 2006, 428(1−2): 148−158.

[13] YANG Yong-qiang, SU Xu-bin, WANG Di, CHEN Yong-hua. Rapid fabrication of metallic mechanism joints by selective laser melting [J]. Journal of Engineering Manufacture, 2011, 225(12): 2249−2256.

[14] JOO B, JANG J, LEE J, SON Y, MOON Y. Selective laser melting of Fe-Ni-Cr layer on AISI H13 tool steel [J]. Transactions of Nonferrous Metals Society of China, 2009, 19: 921−924.

[15] MORGAN R, SUTCLIFFE J, O'NEILL W. Density analysis of direct metal laser re-melted 316L stainless steel cubic primitives [J]. Journal of Materials Science, 2004, 39(4): 1195−2005.

[16] SU Xu-bin, YANG Yong-qiang. Research on track overlapping during selective laser melting of powders [J]. Journal of Materials Processing Technology, 2012, 212(10): 204−207.

基于激光叠层制造的多孔医用植入支架的开发

苏旭彬[1]，杨永强[2]，于　鹏[1]，孙健峰[2]

1. 华南理工大学 材料科学与工程学院，广州 510640；
2. 华南理工大学 机械与汽车工程学院，广州 510640

摘　要：研究多孔医用植入支架的数字化设计和激光叠层制造工艺制备方法。利用 CT 技术和 Pro/Engineer 软件设计出具备个性化特征的多孔人工股骨模型和多孔心血管支架模型，然后采用钛合金粉末材料，由选区激光熔化工艺直接制备出来。结果表明，通过改进支架单元体的结构工艺性，可以避免添加支撑，所制备的多孔支架具有良好的贯通性。同时，若干问题也呈现出来，如单元体的几何精度较差。由于患者具备个体特征，叠层制造工艺所具备的自由设计有利于其在医学上的应用。随着设计、工艺、生物相容性等的进一步研究，将会开发出更多的支架并应用于临床。

关键词：粉末材料；医用植入体；多孔结构；结构工艺性；快速制造

(Edited by CHEN Wei-ping)